



Composite cathode for IT-SOFC: Sr-doped lanthanum cuprate and Gd-doped ceria

Seung Jun Lee, P. Muralidharan¹, Seung Hwan Jo¹, Do Kyung Kim^{*}

Department of Materials Science and Engineering, Korea Advanced Institute of Science and Technology (KAIST), 335 Gwahangno, Yuseong-gu, Daejeon 305-701, Republic of Korea

ARTICLE INFO

Article history:

Received 27 January 2010

Received in revised form 25 March 2010

Accepted 26 March 2010

Available online 2 April 2010

Keywords:

Cathode

Citrate combustion synthesis

$\text{La}_{1.96}\text{Sr}_{0.04}\text{CuO}_{4+\delta}$

Electrochemical performance

IT-SOFCs

ABSTRACT

Composite cathodes were synthesized via a citrate combustion method followed by an organic precipitation method. The cathodes were of K_2NiF_4 -type crystal structure with x wt.% $\text{Ce}_{0.9}\text{Gd}_{0.1}\text{O}_{1.95}$ (CGO)– $(100-x)$ wt.% $\text{La}_{1.96}\text{Sr}_{0.04}\text{CuO}_{4+\delta}$ (LSC), where $x=0, 10, 20$ and 30 . The individual structural phases of the composite cathodes were characterized using a third-generation synchrotron source beamline powder X-ray diffractometer (XRD). The porous grain morphology of the CGO–LSC cathode composite for a symmetrical half-cell was determined from cross-sectional scanning electron microscopy images and elemental line profiles. The composite cathode was made of 20 wt.% CGO–80 wt.% LSC (CL20–80) and was coated onto a $\text{Ce}_{0.9}\text{Gd}_{0.1}\text{O}_{1.95}$ electrolyte. It showed the lowest area specific resistance (ASR) of $0.07 \Omega \text{ cm}^2$ at 750°C . An electrolyte-supported (300 μm thick) single-cell configuration of CL20–80/CGO/Ni–CGO attained a maximum power density of 626 mW cm^{-2} at 700°C . The unique composite composition of CL20–80 demonstrates enhanced electrochemical performance and good chemical compatibility with the CGO electrolyte, as compared with the pure LSC (CL0–100) cathode for IT-SOFCs.

© 2010 Elsevier B.V. All rights reserved.

1. Introduction

Recently, a significant effort has been devoted to the development of intermediate-temperature solid oxide fuel cells (IT-SOFCs) with high power density and working efficiency operating at $500\text{--}800^\circ\text{C}$ [1–4]. With respect to cathode materials, one of the most challenging issues is to obtain low polarization losses related to the interfacial resistances. The development of new, mixed ionic–electronic conducting (MIEC) cathodes demonstrates a potential method to obtain lower interfacial polarization losses. Most of the studies on MIEC cathodes have focused on perovskites, such as BaCoO_3 and LaCoO_3 [5,6].

Recently, a family of compounds of the form $\text{A}_2\text{BO}_{4+\delta}$, with the same type of crystal structure as K_2NiF_4 , has attracted attention as a MIEC cathode due to good characteristics. They show good electronic conductivity attributable to the mixed valence of the B site metal and good oxygen ionic transport properties due to the oxygen overstoichiometry. They also show comparable thermal expansion coefficient (TEC) with solid electrolytes [7,8]. Li et al. [8] reported lower area specific resistances (ASR) and overpotential for the $\text{La}_{1.7}\text{Sr}_{0.3}\text{CuO}_4$ cathode material. However, few papers consider the effect of Sr contents in La site on the cathode properties of La_2CuO_4 . Our preliminary experimental results showed that $\text{La}_{1.96}\text{Sr}_{0.04}\text{CuO}_4$ exhibited the lowest ASR values at all temperatures.

Composite cathodes that include a mixture of the cathode and an ionic conducting material, such as LSM–YSZ, SSC–SDC, PSCC–SDC, and

SBSCO–CGO [2,9–11], have recently gained great interest. This is because they can expand the electrochemically active triple-phase boundaries, at the two-dimensional interface between the electrolyte and the cathode, to the entire zone of the cathode [2,12]. Zhao et al. [7] have reported that composites consisting of $\text{La}_{1.2}\text{Sr}_{0.8}\text{Co}_{0.8}\text{Ni}_{0.2}\text{O}_{4+\delta}$ and $\text{Ce}_{0.9}\text{Gd}_{0.1}\text{O}_{1.95}$ (CGO) exhibit lower interfacial polarization resistances, as compared with those of pure $\text{La}_{1.2}\text{Sr}_{0.8}\text{Co}_{0.8}\text{Ni}_{0.2}\text{O}_{4+\delta}$. It is well-known that cobalt in the cathodes facilitates high oxygen-ion diffusion and surface exchange coefficients, which leads to high cathode performance. However, wide usage of cobalt-containing cathodes is limited by high cost, toxicity and TEC. In addition, nickel-containing oxides experience phase instability problems. Therefore, this investigation is focused on alternative CGO– $\text{La}_{1.96}\text{Sr}_{0.04}\text{CuO}_{4+\delta}$ composites that may be a potential candidate as a cathode material for IT-SOFC.

In this study, homogeneous composite cathodes were synthesized and area specific resistances (ASR) were studied by an electrochemical impedance spectroscopy technique. The homogeneous composite cathodes consisted of x wt.% $\text{Ce}_{0.9}\text{Gd}_{0.1}\text{O}_{1.95}$ (CGO)– $(100-x)$ wt.% $\text{La}_{1.96}\text{Sr}_{0.04}\text{CuO}_{4+\delta}$ (LSC), where $x=0, 10, 20$ and 30 . Single-cell performances of the pure LSC and CL20–80 composite cathodes were also investigated.

2. Experimental

$\text{La}_{1.96}\text{Sr}_{0.04}\text{CuO}_{4+\delta}$ powder was synthesized via citrate combustion (CAC) using analytical grade $\text{La}(\text{NO}_3)_3 \cdot 6\text{H}_2\text{O}$ (>99.99%), $\text{Sr}(\text{NO}_3)_2$ (99+%) $\text{Cu}(\text{NO}_3)_2 \cdot 2.5\text{H}_2\text{O}$ (98%), and citric acid (99%). The CAC method had been described in detail in our previous work [3]. The crystalline $\text{La}_{1.96}\text{Sr}_{0.04}\text{CuO}_{4+\delta}$ powder was obtained through calcination at 900°C for 10 h.

* Corresponding author. Tel.: +82 42 350 4118; fax: +82 42 350 3310.

E-mail address: dkkim@kaist.ac.kr (D.K. Kim).

¹ Equal contribution of work.

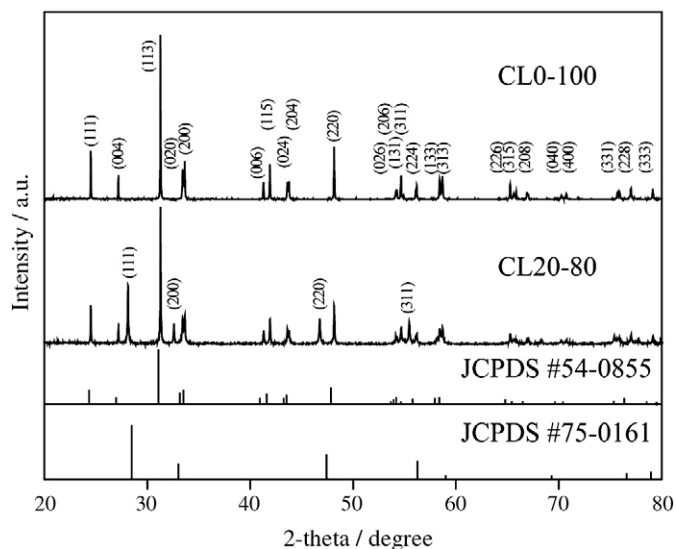


Fig. 1. Synchrotron XRD patterns of the CL0–100 and CL20–80 powders calcined at 900 °C for 10 h and compared with the JCPDS data of CGO and LSC.

Stoichiometric amounts of $\text{Ce}(\text{NO}_3)_3 \cdot 6\text{H}_2\text{O}$ (99.9%) and $\text{Gd}(\text{NO}_3)_3 \cdot 6\text{H}_2\text{O}$ (99.9%) were dissolved in 50 ml of ethanol to form the calculated x wt.% of $\text{Ce}_{0.9}\text{Gd}_{0.1}\text{O}_{1.95}$ in the composite. To the above solution, $(100-x)$ wt.% of calcined LSC powder was dispersed under sonication for 2 h. $(\text{C}_2\text{H}_5)_2\text{NH}$ (diethylamine, 99.9%) precipitant was used to precipitate the CGO in the presence of LSC in order to form the composite. The composite powders obtained were dried at 80 °C for 12 h and calcined at 900 °C for 10 h. The CGO–LSC composite cathodes with different x wt.% of CGO and LSC powders (CL), where $x = 0, 10, 20$

and 30, were denoted using sample codes: CL0–100, CL10–90, CL20–80 and CL30–70.

The phases of the synthesized composite powders were characterized with a third-generation synchrotron powder X-ray diffractometer (XRD) from the 8C2 station beam line, with $\text{Cu-K}\alpha$ radiation ($\lambda = 1.549 \text{ \AA}$) at the Pohang Light Source (PLS) in Korea. The cross-sectional microstructure of the cathode coated onto the CGO electrolyte was characterized using a scanning electron microscope (FE-SEM Philips XL30 FEG) and elemental line profiles.

The symmetrical half-cells, with a CGO–LSC/CGO/CGO–LSC configuration, were fabricated by screen-printing, as described in our previous paper [3]. ASRs were characterized using 3-probe ac impedance spectroscopy (Solartron 1260 impedance/Gain-phase analyzer) in a frequency range of 10^6 to 10^{-2} Hz as a function of temperature (600–800 °C) in flowing air.

Single-cells were fabricated by screen-printing the anode in NiO–CGO on one side of the dense CGO electrolyte pellet. They are then sintered at 1300 °C for 2 h, followed by the cathode coating on the opposite side [3]. The single-cells were then sintered at 900 °C for 4 h. A Keithley 2400 source meter was used to measure I – V polarization under flowing humidified H_2 ($\sim 3\%$ H_2O) as a fuel, and in air as an oxidant.

3. Result and discussions

Fig. 1 shows the synchrotron source XRD patterns of CL0–100 and the CL20–80 cathodes, calcined at 900 °C for 10 h. The pattern of pure CL0–100 exhibits pure phase and high crystallinity, with no peaks attributed to detected impurities. All the diffraction peaks of $\text{La}_{1.96}\text{Sr}_{0.04}\text{CuO}_{4+\delta}$ can be indexed based on the JCPDS card # 54-0855, with an orthorhombic K_2NiF_4 -type structure, as shown in Fig. 1. The unit cell parameters for $\text{La}_{1.96}\text{Sr}_{0.04}\text{CuO}_{4+\delta}$ are $a = 5.345 \text{ \AA}$, $b = 5.383 \text{ \AA}$ and $c = 13.188 \text{ \AA}$. The cell volume is 379.50 \AA^3 . The pattern of the CL20–80

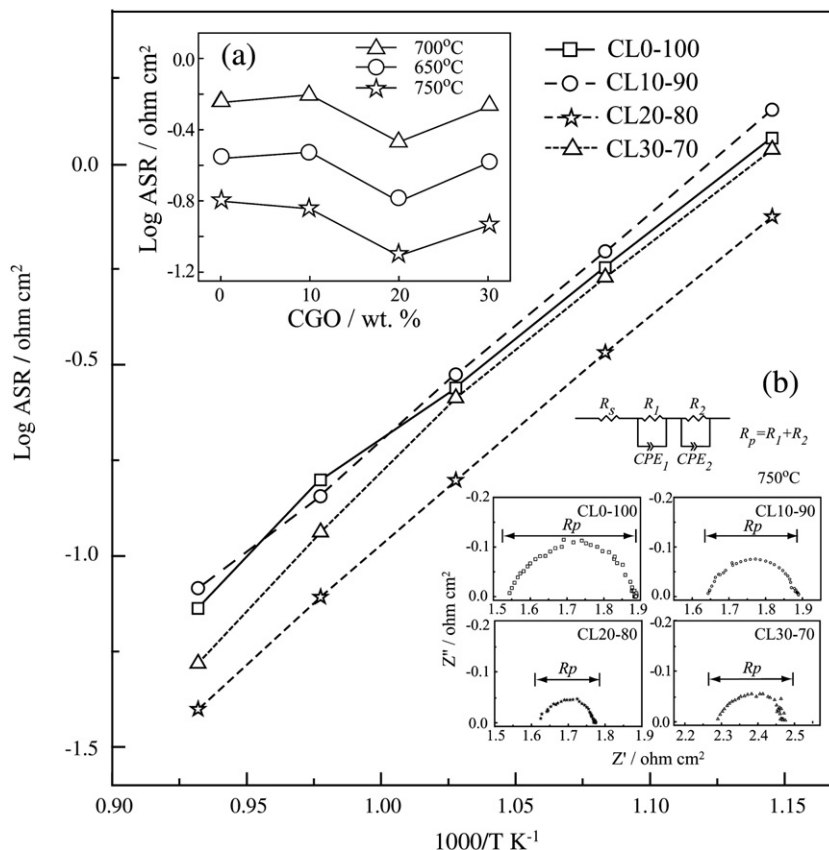


Fig. 2. Arrhenius plots of log ASR for the symmetrical half-cells of different wt.% CL/CGO at the interface, measured in air. The inset (a) shows the ASR values vs. wt.% CGO in the composites. The inset (b) shows the impedance spectra of different wt.% CGO-containing composites at 750 °C.

composite shows the presence of indexed peaks corresponding to CGO and $\text{La}_{1.96}\text{Sr}_{0.04}\text{CuO}_{4+\delta}$ without any other secondary phases. The synchrotron XRD results indicate that CGO and $\text{La}_{1.96}\text{Sr}_{0.04}\text{CuO}_{4+\delta}$ have a good chemical compatibility as a homogeneous composite, without forming any solid-solution.

In Fig. 2, the calculated log ASR of pure CL0–100 and CL composites with different wt.% of CGO shows the interface resistances as a function of temperature. The two insets (a) and (b) in Fig. 2 show the plot of ASR values vs. wt.% of CGO in the CL composites and the impedance spectra for the symmetrical half-cells fabricated with pure CL0–100 and CL composites with different wt.% of CGO, respectively. The resistivity ($R_p = R_1 + R_2$) was obtained by fitting the impedance spectrum with an equivalent circuit model (inset (b) in Fig. 2) using the nonlinear least squares fitting program of the Z-view software. The intercept of the semicircle on the real axis in the high-frequency region represents the total ohmic resistivity (R_s) of the electrolyte. The radius of the arc between the two intercepts in the high- and low-frequency regions on the real axis corresponds to the polarization resistivity (R_p) of the cathodes. In Fig. 2, the CL20–80 composite cathode on the $\text{Ce}_{0.9}\text{Gd}_{0.1}\text{O}_{1.95}$ (CGO) electrolyte can be seen to have an ASR value of $0.07 \Omega \text{ cm}^2$ at 750°C , which is lower than the value for the pure CL0–100 cathode. The inset (a) clearly reveals that the CL20–80 composite possesses the lowest ASR values at various temperatures.

In composite cathodes, the electrochemical reaction (ECR) zone is generally recognized to be expanded from the limits of the two-dimensional interface between the electrolyte and the cathode to the entire ECR area of the cathode. This significantly improves cathode performance [2,12]. As a result, the high ionic conductivity of CGO in the CL composite cathodes may facilitate oxygen conduction paths and greatly expand the ECR sites. This would result in an improvement of the performance under IT-SOFC operating conditions [2,12].

These effects reflect a decrease in R_p due to a reduction in charge transfer resistance (R_2).

The SEM and elemental line profiles in Fig. 3a–d show the cross-sectional views of an interface between the CL20–80 cathode and the CGO electrolyte substrate, which were sintered at 900°C for 4 h. The SEM images show thin layers of cathodes ($\sim 17 \mu\text{m}$ thick) with a highly porous morphology that ensures good gas diffusion. The images also display the presence of inter-connectivity at interfaces between the porous cathode and the densified electrolyte (Fig. 3d). Fig. 3c shows that the composite cathode consists of homogeneously-distributed, nano-sized ($\sim 100 \text{ nm}$) and spherical CGO particles (indicated by arrows in Fig. 3c–d) on the surface of the bottle-neck shaped LSC particles ($\sim 1 \mu\text{m}$). The elemental line profiles in Fig. 3b show the distribution of elements Gd, La, Ce, Cu and Sr in the cathode and electrolyte regions. These results confirmed the homogeneous distribution of composite particles. They also show the presence of elements in limited regions without any inter-penetration of the elements, which is also evident from the synchrotron XRD patterns (Fig. 1). The high-magnification image of the interfacial region in Fig. 3d demonstrates that the homogeneously-distributed, nano-sized and spherical CGO particles on the large LSC particles adhere to the densified CGO electrolyte. This typical morphology may be one of the reasons for reduced cathode polarization during the oxygen reduction reaction. This suggests an explanation for enhancement of the electrochemical performance of CL20–80 compared with pure CL0–100.

The electrochemical performances are shown in Fig. 4, with the CGO electrolyte-supported single-cell configurations of CL0–100 or CL20–80/CGO/Ni-CGO in the temperature range of $550\text{--}700^\circ\text{C}$. The inset table in Fig. 4 represents the maximum power densities of pure CL0–100 (329 mW cm^{-2}) and CL20–80 (626 mW cm^{-2}) at 700°C . These are comparable to the data found in the literature [7,13,14]. These results

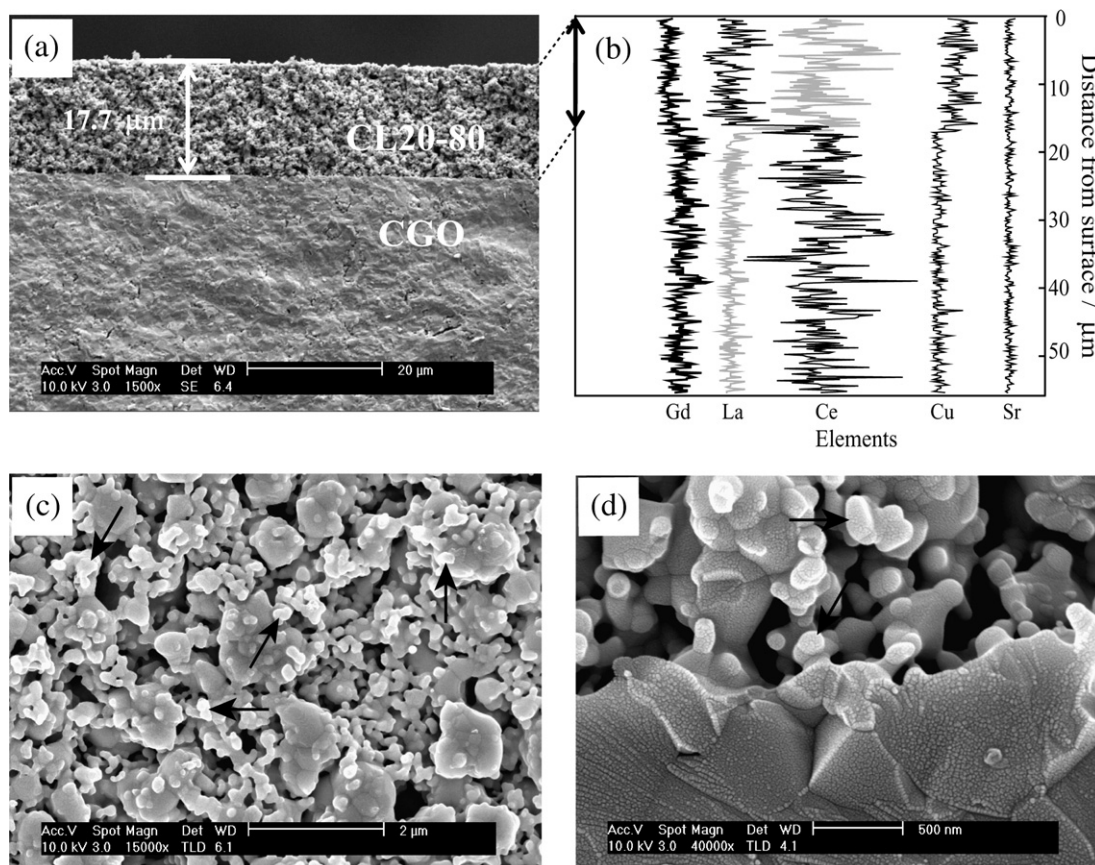


Fig. 3. SEM images of the cross-section of an interface between the CL20–80 cathode and CGO electrolyte substrate (a) low-magnification, (b) line profiles, (c) high-magnification of cathode (arrows indicate the CGO particles) and (d) high-magnification image of interface.

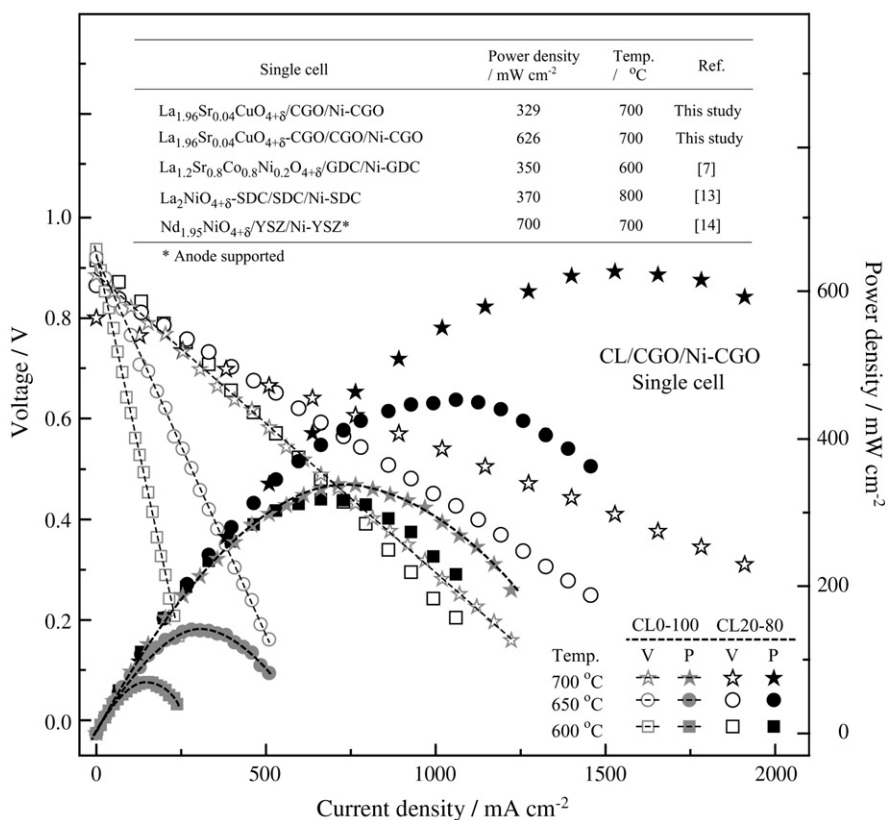


Fig. 4. Electrochemical performance of the CL0-100 and CL20-80/CGO/Ni-CGO single-cells under humidified H₂ fuel and air oxidant at different temperatures.

demonstrate that the CL20-80 composite cathode exhibits higher performance than that of pure CL0-100 in the intermediate-temperature regime. The enhanced electrochemical performance of the CL20-80 composite cathode was attributed to the effects of the homogeneous CGO particle distribution, fine pore structure and good inter-connectivity between the particles of each solid phase. This has yielded large triple-phase boundary areas accessible for efficient oxygen reduction processes and fast charge transport.

4. Conclusions

Different wt.% CGO-containing composite cathodes (CL0-100 to CL30-70) were synthesized via CAC, followed by the precipitation procedure. The ASR values were improved by mixing nano-sized CGO and LSC particles to form CL composite cathodes. The maximum power density of the electrolyte-supported single-cell CL20-80/CGO/Ni-CGO attained 626 mW cm⁻² at 700 °C. The homogeneous CL composites with distributed nano-sized CGO particles on LSC were advantageous for the electrochemical performance. In addition, the CL composites are proving to be a potential cathode in IT-SOFC due to their low expense, low toxicity and good chemical compatibility.

Acknowledgements

This work was financially supported by the Priority Research Centers Program through the National Research Foundation of Korea

(NRF) (No. 2008-0062204), Center for ERC Program (2008-0062206) and by Brain Korea 21 (BK21) program funded by Korea government (MSET). The authors thank the Pohang Light Source, Korea for extending the synchrotron XRD for characterization.

References

- [1] W. Zhou, R. Ran, Z. Shao, W. Zhuang, J. Jia, H. Gu, W. Jin, N. Xu, *Acta Mater* 56 (2008) 2687.
- [2] C. Zhu, X. Liu, D. Xu, D. Wang, D. Yan, L. Pei, T. Lü, W. Su, *J. Power Sources* 185 (2008) 212.
- [3] S.H. Jo, P. Muralidharan, D.K. Kim, *Electrochem. Commun.* 11 (2009) 2085.
- [4] S.H. Jo, P. Muralidharan, D.K. Kim, *Electrochim. Acta* 54 (2009) 7495.
- [5] Z. Shao, S.M. Haile, *Nature* 431 (2004) 170.
- [6] A. Esquirol, N.P. Brandon, J.A. Kilner, M. Mogensen, *J. Electrochem. Soc.* 151 (2004) A1847.
- [7] F. Zhao, X. Wang, Z. Wang, R. Peng, C. Xia, *Solid State Ionics* 179 (2008) 1450.
- [8] Q. Li, H. Zhao, L. Huo, L. Sun, X. Cheng, J.-C. Grenier, *Electrochem. Commun.* 9 (2007) 1508.
- [9] J. Piao, K. Sun, N. Zhang, S. Xu, *J. Power Sources* 175 (2008) 288.
- [10] C. Xia, W. Rauch, F. Chen, M. Liu, *Solid State Ionics* 149 (2002) 11.
- [11] J.H. Kim, M. Cassidy, J.T.S. Irvine, J. Bae, *J. Electrochem. Soc.* 156 (2009) B682.
- [12] H. Gu, H. Chen, L. Gao, L. Guo, *Electrochim. Acta* 54 (2009) 7094.
- [13] D. Pérez-Coll, A. Aguadero, M.J. Escudero, L. Daza, *J. Power Sources* 192 (2009) 2.
- [14] C. Lalanne, F. Mauvy, E. Siebert, M.L. Fontaine, J.M. Bassat, F. Ansart, P. Stevens, J.C. Grenier, *J. Eur. Ceram. Soc.* 27 (2007) 4915.